Fusion Engineering and Design 192 (2023) 113629

Contents lists available at ScienceDirect

Fusion Engineering and Design

journal homepage: www.elsevier.com/locate/fusengdes

# Conceptual design of the next generation of W7-X divertor W-target elements

J. Boscary [a,*], G. Ehrke [b], P. Frosi [f], P. Junghanns [a], B. Končar [e], B. Mendelevitch [a], D. Naujoks [b], R. Neu [a], M. Richou [c], L. Selan [e], J. Tretter [a], Z. Wang [a], J.H. You [a], K. Zhang [d]

[a] Max-Planck-Institut für Plasmaphysik, Boltzmannstr. 2, Garching 85748, Germany
[b] Max-Planck-Institut für Plasmaphysik, Wendelsteinstr. 1, Greifswald 17498, Germany
[c] CEA IRFM, Saint-Paul-Lez-Durance, 13108, France
[d] Karlsruhe Institute of Technology, Karlsruhe 76131, Germany
[e] Jožef Stefan Institute, Reactor Engineering Division, Jamova 39, Ljubljana 1000, Slovenia
[f] ENEA Frascati, Dept. of Fusion and Technology for Nuclear Safety, via E. Fermi 45, Frascati 00044, Italy

ARTICLE INFO

*Keywords:*
Stellarator
Wendelstein 7-X
Plasma facing component
Divertor

ABSTRACT

The stellarator Wendelstein 7-X (W7-X) will start operation with an actively water cooled divertor made of target elements armored with CFC (Carbon Fiber Reinforced Carbon) NB31 tiles in 2022. The next step (> 2030) is the installation of a metallic water cooled divertor. Research activities have been launched supported by EUROfusion to develop the next generation of metallic target element. The purpose of the conceptual design is to prepare the first prototyping phase. Stationary loading and water cooling conditions are: 10 MW/m$^2$, $T_{in}$=30°C, $P_{static}$=1 MPa, $V_{axial}$=9m/s. Similar to the current divertor, the heat sink is made of CuCrZr . Two kinds of armor materials are considered: pure tungsten and W3.5Ni1.5Cu heavy alloy. One of the main constraints is to keep a weight similar to the CFC design to limit the divertor module weight for assembly. The first analyzed model is a straightforward adaptation of the simplest geometry of a CFC element. Thermal calculations show that the maximal temperatures remain within acceptable limits and 3.5 mm armor layer should be considered as the upper thickness limit. By reducing the distance between coolant and loaded surface the need for swirl flow should be assessed in more details. In addition to modelling, first trials for the industrial manufacturing of the CuCrZr heat sink, armor, bonding procedure have been launched.

## 1. Introduction

The stellarator Wendelstein 7-X (W7-X) located in Greifswald, Germany, will start operation with the full set of actively water cooled plasma facing components in 2022. W7-X is equipped with a divertor which has a total surface of about 25m$^2$ made of ten discrete divertor units: a lower loaded surface designed for stationary maximal loads up to 1 MW/m$^2$ with a surface of about 6 m$^2$ and a highly heat loaded surface designed for stationary maximal loads up to 10 MW/m$^2$ with a surface of about 19 m$^2$ [1]. The highly loaded surface is made of 890 target elements [2]. A target element is made of a CuCrZr copper alloy heat sink armored with carbon fibre reinforced carbon CFC NB31 tiles.

In order to investigate the performance of the HELIAS (HELIcal-axis Advanced Stellarator) concept with reactor relevant plasma facing material, the installation of all-metallic plasma facing components is foreseen in W7-X after the extensive exploitation of the presently installed divertor (> 2030). The lessons learnt from the analyses of the production of the CFC target elements showed that the efforts required to deliver such components have been underestimated. Therefore research activities have been launched at an early stage in the frame of the EUROfusion work package WP-DIV to develop the next generation of metallic target elements.

## 2. Conceptual design

Today the final geometry and surface of the next metallic divertor are not defined. The present available set of experimental data refer to the first phase of W7-X operation (OP1.1 & 2) [3] with a non water cooled divertor [4] but with the same geometry as the water cooled divertor. Therefore, it is assumed at the present stage that the next divertor

* Corresponding author.
*E-mail address:* jean.boscary@ipp.mpg.de (J. Boscary).

https://doi.org/10.1016/j.fusengdes.2023.113629
Received 27 September 2022; Received in revised form 18 January 2023; Accepted 1 March 2023
Available online 7 March 2023

surface will be a straightforward evolution of the present surface, which will be confirmed or not in the future. A first necessary modification, which was clearly identified in OP1.2, is to provide a full highly loadable divertor surface without the lower loaded part of the current divertor.

The integration in the present W7-X environment significantly dictates the target element design. To reduce investment, modifications of the water supply outside the machine have to be minimized. The water cooling loop design and characteristics as well as the water pump characteristics are planned to remain unchanged. The feeding cooling circuits of the divertor cross the cryostat and the plasma vessel wall through ad hoc flanged penetrations called "plug-ins" installed in dedicated ports. The plug-ins provide for the vacuum boundary between the plasma chamber and the torus hall atmosphere. The plug-ins used for cooling the lower loaded surface will have to be adapted to allow for higher cooling performance in this area. The position of the plug-ins determine the location of the water inlet and outlet at the same end of the target element. Basically the divertor surface is made of 2D thick consecutive elements joining two concentric circles of different diameters, which follows the twisted plasma surface. The results of the discretization of the divertor surface in individual elements produced a trapezoidal outer shaping along and across the element.

As shown in Fig. 1, the divertor surface includes a pumping gap with cryo-vacuum pumps [5] to allow for screening impurities and efficient control of plasma density.

As a consequence a protection of the ends of the target elements is needed which defines the geometrical boundary of the pumping gap. The maximal allowable local heat flux at this location has been specified in the range of 2-5 MW/m$^2$ on the basis of experimental high heat flux testing with a design constrained by manufacturing process conditions [6]. This solution limits positioning flux strike lines as close as possible to the gap. A requested improvement of the design to reach performance close to the surface heat flux of 10 MW/m$^2$ has to be investigated in the future. This point shows that the monobloc design [7] for W7-X is not well adapted to the W7-X environment. W7-X has decided to keep the same value of the maximal top surface heat flux as for the CFC design of 10 MW/m$^2$ in stationary conditions. In transient conditions and based on peaked profiles measured for high iota in OP1.x, a maximal peak value of 15 MW/m$^2$ for 1-3 seconds has been set. Cooling conditions that define the working point of the target element remain the same as for CFC: local axial velocity of 9 m/s, static pressure of 1 MPa, maximal inlet temperature of 30°C. For the divertor cooling loop, main features are unchanged: maximal dynamic pressure of 1.4 MPa, maximal water temperature increase of 50K. Another requirement is a smooth shape of the whole divertor surface; the solution retained for the CFC element was the individual machining of the element before positioning in the modules [8]. Technological solutions to shape the metallic surface of the W7-X need to be developed and validated. One of the most important point identified during the assembly phase of the divertor was the difficulty to transport and position the target module in the restricted available space in the plasma vessel. The maximal weight of the CFC modules of 70 kg has been set as a limit with the goal to be reduced. The design of the module is not considered in this paper.

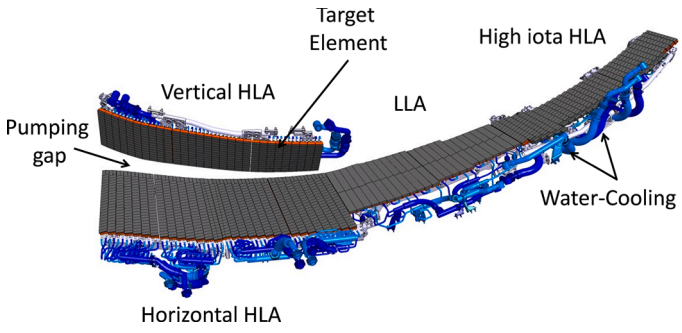


**Fig. 1.** Main target areas of one divertor unit. The divertor is an open structure with the horizontal and vertical targets, which define the main pumping gap (HLA: Higher Loaded Area, LLA: Lower Loaded Area).

## 3. Thermal simulation and analysis

The conservative model selected for thermal simulations is very close to the CFC design. The heat sink is made of CuCrZr with a Ø9 mm cooling channel. The CFC tiles are replaced by W or W-alloy tiles with two tiles instead of one tile across the element.

The selected geometry is an adaptation of the type 4S of CFC elements (Fig. 2). A 2 mm interlayer made of copper is placed between armor and heat sink to accommodate the mismatch between armor and heat sink. At this stage, the bonding technology is not selected but this design is assumed to be quite representative of one of a possible technological solution. Water cooling conditions are: 9 m/s axial velocity; 50°C bulk temperature; 1 MPa pressure. These values are used to calculate the heat transfer coefficient at the wall of the cooling channel based on the Nukiyama curve in sub-cooled conditions [9], The different possible regimes, i.e. forced convection [10], transition to partial sub-cooled to fully developed nucleate boiling [11] are obtained from correlations adapted to the specified conditions, which have been experimentally validated [12]. Same approach was adopted for the critical heat flux [13,14]].

Calculations have been performed with ANSYS version 19. Table 1 lists the selected calculated cases. The need for the installation of the twisted tape in the straight parts of the cooling channel is also investigated due to its high dynamic pressure. In case of swirl flow, the twisted tape made of stainless steel has a twist ratio of 2 and a thickness of 1 mm. Two armor materials are considered: pure tungsten and W3.5Ni1.5Cu [15].

W-alloys are considered due to their foreseen better machinability with the disadvantage of a lower thermal conductivity and a reduction in allowed surface temperature.

The purpose of the simulation is to get the temperature field distribution of the tiles, heat sink, and wall of the cooling channel. Fig. 3 illustrates the results of the thermal calculation performed for case 3S.

Table 2 and 3 summarize the results of the calculations for the different cases 1-5.

The simple criteria are defined as follows: (1) the saturation temperature for 1 MPa water pressure for the wall of the cooling channel, (2) for the heat sink, the temperature at which CuCrZr starts losing strength [16], (3) for the surface, the material melting/recrystallisation temperatures (with some safety margin) [15]. The same kind of simulation with ANSYS CFD (Computational Fluid Dynamics) has been also performed in parallel to analyze the impact of the water flow on the temperature distribution [17]. Table 2 shows that the maximal temperatures

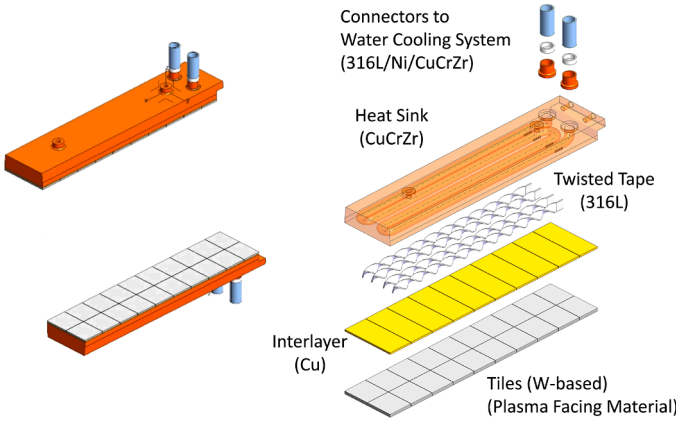


**Fig. 2.** CAD view of the adapted type 4S element: length = 250 mm; width = 56 mm; tile thickness = 3.5 mm. The different parts of an element are shown.

**Table 1**
Selected loading conditions - A: pure tungsten; B: W3.5Ni1.5Cu – S: swirl, NS: no swirl

| Cases | Tile Material | Power Load [MW/m$^2$] | Profile |
|---|---|---|---|
| 1S/NS | A | 10 | Steady-state, flat |
| 2S/NS | A | 10 | Steady-state, peaked |
| 3S/NS | B | 10 | Steady-state, flat |
| 4S/NS | B | 10 | Steady-state, peaked |
| 5S/NS | B | 15 | Transient 3s., peaked |

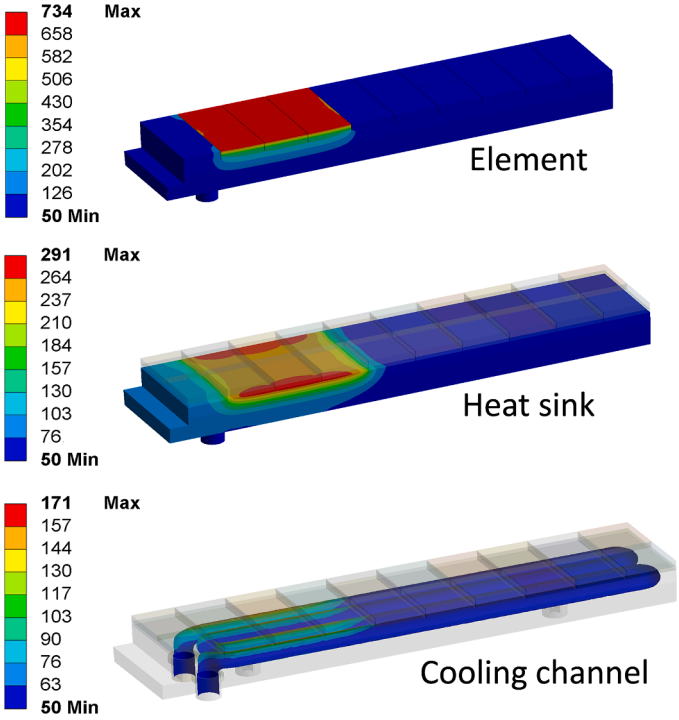


**Fig. 3.** . Example of temperature distribution for case 1 (heat flux = 10 MW/m$^2$)

**Table 2**
Calculated maximal temperature T for the different cases defined in Table 1 with swirl

| T [°C] | 1 | 2 | 3 | 4 | 5 | Criteria |
|---|---|---|---|---|---|---|
| Surface W | 601 | 543 | | | | 1300 |
| Surface W3.5Ni1.5Cu | | | 735 | 684 | 985 | 900 |
| Heat sink | 296 | 261 | 291 | 322 | 359 | 450 |
| Channel | 172 | 156 | 172 | 164 | 204 | 180 |

**Table 3**
Calculated maximal temperature T for the different cases defined in Table 1 without swirl

| T [°C] | 1 | 2 | 3 | 4 | 5 | Criteria |
|---|---|---|---|---|---|---|
| Surface W | 687 | 600 | | | | 1300 |
| Surface W3.5Ni1.5Cu | | | 803 | 740 | 1048 | 900 |
| Heat sink | 368 | 309 | 357 | 373 | 422 | 450 |
| Channel | 237 | 219 | 253 | 233 | 295 | 180 |

are below the criteria, except slightly for case 5. Table 3 illustrates the need for a swirl flow to keep the heat transfer regime in forced convection or at least allowing local starting of nucleate boiling. The armor thickness of 3.5 mm should be considered as the upper thickness limit. In this first calculation, the thickness is constant and does not consider the surface shaping. As for the current CFC divertor, the range of armor thickness is defined by the whole divertor surface shaping, acceptable steps between neighboring elements, operation conditions, tolerances (process, positioning, measurement) for the surface production, which are presently not well defined. By reducing the distance between coolant and loaded surface the need for swirl flow should be assessed in more details while taking the required thermo-mechanical stability of the component during the production and in operation into account.

## 4. Investigation of possible technological solutions

Development of the target elements requires an extensive prototyping phase to minimize the risks for the industrial production together with an adequate testing programme: high heat flux testing (maximal performance, thermal cycling), validation of non-destructive examination methods. In the present case, major technological solutions to be developed and validated are indicated in the schematic of Fig. 4.

❶ covers three topics: (1) selection of material(s) compatible with plasma operation, bonding technology and surface shaping (2) shape selection, free form as CFC or successive plane facets (3) surface process selection, milling or spark erosion for example. ❷ is the most important topic which defines not only the performance but also the lifetime of the divertor. The past decade has seen the development of different technological solutions for the flat tile design worldwide for use in different experimental fusion machines. For the upper divertor of EAST, cast W-tiles with a Cu-interlayer are joined by HIPping (Hot Isostatic Pressure) on a CuCrZr heat sink [18,19]. For the divertor ITER dome, cast W-tiles with a Cu-interlayer are brazed on a CuCrZr heat sink [20]. Bonding technologies also developed for the monobloc design for ITER and WEST such as hot isostatic pressing should be assessed [21]. These selected references amongst many others show the portfolio of available different developed technologies; however, as shown for the CFC target elements, the implementation to the W7-X geometry requires the validation of the technologies by testing [22]. ❸ CuCrZr as material heat sink is the most appropriate for W7-X. The manufacturing process of the heat sink for the CFC solution by electron beam welding of two half parts was very demanding and a better design and technological solution has to be developed. Two different approaches are followed. A conservative approach is to drill the channels in a CuCrZr plate and then join the different channels, which remains not trivial. First test sections have been produced. Drilling non parallel channels with thin neighboring wall thickness over a maximal length of about 600 mm needs additional development. Samples are planned to be produced in collaboration with TUM (Technical University of Munich) to analyze the joining of parts made of CuCrZr by diffusion bonding for the W7-X geometry. A quite innovative approach is to consider the fast development of the additive manufacturing of CuCrZr [23] as an opportunity to develop also new cooling channel design. A collaboration with the Fraunhofer Institute of Augsburg, Germany has been launched on this topic [24].

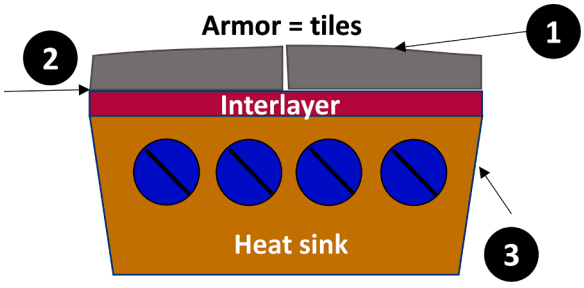


**Fig. 4.** Schematic cross-section of a target element with technological topics to be addressed: ❶: armor material and shaping, ❷: bonding tiles/heat sink, ❸: heat sink design

## 5. Conclusion

Development activities of the next generation of target elements for the next metallic water cooled divertor of W7-X started in the frame of the EUROfusion work package WP-DIV. The purpose of the conceptual design is to define the main features of the first prototypes. The approach is very conservative with a straightforward adaptation of the CFC target elements by replacing the armor material and reducing the size and thickness (3.5 mm) of the tiles to keep the total weight of the element unchanged. Pure tungsten but also W heavy alloy are investigated to take into account at a very preliminary stage the efforts required for the demanding production of the final shape of the divertor surface. Simple thermal simulations set the main geometrical features based on criteria defined for the maximal temperature. The armor thickness of 3.5 mm should be considered as the upper thickness limit. Activities have been also launched to assess different technological solutions: drilling of the cooling channel, CuCrZr heat sink production by additive manufacturing. The next major step is the selection of different bonding technologies between heat sink and armor to be assessed for the W7-X needs.

## Declaration of Competing Interest

The authors declare that they have no known competing financial interests or personal relationships that could have appeared to influence the work reported in this paper.

## Data availability

The authors are unable or have chosen not to specify which data has been used.

## Acknowledgment

This work has been carried out within the framework of the EUROfusion Consortium, funded by the European Union via the Euratom Research and Training Programme (Grant Agreement No 101052200 — EUROfusion). Views and opinions expressed are however those of the author(s) only and do not necessarily reflect those of the European Union or the European Commission. Neither the European Union nor the European Commission can be held responsible for them.

## References

[1 J. Boscary, et al., Completion of the production of the W7-X divertor target modules, Fusion Eng. Des. 166 (2021), 112293, https://doi.org/10.1088/1741-4326/ab03a7.
[2] J. Boscary, et al., Summary of the production of the divertor target elements of Wendelstein 7-X, Fusion Eng. Des. 124 (2017) 348–351, https://doi.org/10.1016/j.fusengdes.2017.03.084.
[3] T.S. Pedersen, et al., First divertor physics studies in Wendelstein 7-X, Nucl. Eng. 59 (2019), 096014, https://doi.org/10.1088/1741-4326/ab280f.
[4] A. Peacock, et al., Progress in the design and development of a test divertor (TDU) for the start of W7-X operation, Fusion Eng. Des. 84 (2009) 1475–1478, https://doi.org/10.1016/j.fusengdes.2009.01.053.
[5] G. Ehrke, et al., Design and Manufacturing of the Wendelstein 7-X Cryo-Vacuum Pump, Fusion Eng. Des. 146 (2019) 2750–2760, https://doi.org/10.1016/j.fusengdes.2009.05.020.
[6] J. Boscary, et al., Design improvement of the target elements of Wendelstein 7-X divertor, Fusion Eng. Des. 87 (2012) 1453–1456, https://doi.org/10.1016/j.fusengdes.2012.03.034.
[7] B. Riccardi, et al., Progress of the EU activities for the ITER divertor inner vertical target procurement, Fusion Eng. Des. 146 (2019) 1524–1527, https://doi.org/10.1016/j.fusengdes.2019.02.120.
[8] P. Junghanns, et al., Experience gained with the 3D machining of the W7-X HHF divertor target elements, Fusion Eng. Des. (2015) 1226–1230, https://doi.org/10.1016/j.fusengdes.2014.11.018, 98–99.
[9] S. Nukiyama, The maximum and minimum values of the heat transfer Q transmitted from metal to boiling water under atmospheric pressure, Int. J. Heat Transfer 9 (1966) 1419–1433.
[10] V. Gnielinski, New equations for heat and mass transfer in turbulent pipe and channel flow, Int. Chemical Eng. Vol. 16 (2) (1976) 359–368.
[11] A.E. Bergles, W.M. Rohsenow, The determination of forced convection surface boiling heat transfer, J. Heat Transfer ASME Trans. (1964) 365–372.
[12] J. Boscary, PhD report, Transfert thermique et flux critique dans un écoulement hélicoidal en tube chauffé asymétriquement, EUR-CEA-FC-1602, 1997.
[13] L. S. Tong, A phenomenological study of critical heat flux, ASME 75-HT-68, 1975.
[14] J. Boscary, J. Fabre, J. Schlosser, Critical heat flux of water subcooled flow in one-side heated swirl tubes, Int. J. Heat Mass Transfer 42 (1999) 287–301.
[15] R. Neu, et al., Investigations on tungsten heavy alloys for use as plasma facing material, Fusion Eng. Des. 124 (2017) 450–454, https://doi.org/10.1016/j.fusengdes.2017.01.043.
[16] M. Merola, et al., Influence of the manufacturing heat cycles on the CuCrZr properties, J Nuclear Materi. (2002) 677–680, 307–311.
[17] B. Koncar et al., Numerical analysis of boiling effects in cooling channels of W7-X divertor target element, this conference.
[18] Q Li, et al., Development and application of W/Cu flat-type plasma facing components at ASIPP, Phys. Scr. 2017 (2017), 014020.
[19] M. Missirlian, et al., Qualification and post-mortem investigation of actively cooled tungsten flat tile mock-ups for WEST divertor, Fus. Eng. and Des. 136 (2018) 403–409, https://doi.org/10.1016/j.fusengdes.2018.02.063.
[20] N. Litunovsky, et al., Development of the armoring technique for ITER divertor dome, Fus. Eng. and Des. 86 (2011) 1749–1752, https://doi.org/10.1016/j.fusengdes.2011.02.050.
[21] M. Richou, et al., Acceptance tests of the industrial series manufacturing of WEST ITER-like tungsten actively cooled divertor, Phys. Scr. 96 (2021), 124029, https://doi.org/10.1088/1402-4896/ac2657.
[22] H. Greuner, et al., Results and consequences of high heat flux testing as quality assessment of the Wendelstein 7-X divertor, Fusion Eng. Des. 88 (2013) 581–584, https://doi.org/10.1016/j.fusengdes.2013.05.044.
[23] C. Salvan, et al., CuCrZr alloy produced by laser powder bed fusion: Microstructure, nanoscale strengthening mechanisms, electrical and mechanical properties, Mater. Sci. Eng. A 826 (2021), 141915, https://doi.org/10.1016/j.msea.2021.141915.
[24] https://www.igcv.fraunhofer.de/.